Acta Crystallographica Section D
Biological Crystallography
ISSN 0907-4449

Structure determination of GGA-GAE and γ1-ear in complex with peptides: crystallization of low-affinity complexes in membrane traffic

Yusuke Yamada,[a,b] Michio Inoue,[a,b] Tomoo Shiba,[a] Masato Kawasaki,[a] Ryuichi Kato,[a,b] Kazuhisa Nakayama[c] and Soichi Wakatsuki[a,b]*

[a]Structural Biology Research Center, Photon Factory, High Energy Accelerator Research Organization, Japan, [b]The Graduate University for Advanced Studies, 1-1 Oho, Tsukuba, Ibaraki 305-0801, Japan, and [c]The Graduate School of Pharmaceutical Sciences Kyoto University, Yoshida, Sakyo-ku, Kyoto 606-8501, Japan

Correspondence e-mail: soichi.wakatsuki@kek.jp

Received 9 August 2004
Accepted 28 March 2005

© 2005 International Union of Crystallography
Printed in Denmark – all rights reserved

Crystallization of protein–protein complexes is an important step in the studies of biological functions of proteins. However, weak and transient, even though specific, interactions often present difficulties in crystallization of protein complexes due to the heterogeneity of the sample mixture. For example, the γ1-ear domain of the AP-1 complex and the GAE domain of GGA1, responsible for the interaction with accessory proteins involved in vesicular transport, are known to interact with target proteins with affinities of the order of 1–100 μ*M*. Such low affinities have hampered crystallization trials of the complexes. To overcome this problem, the γ1-ear and GAE domains were first co-crystallized with excess amounts of the peptides. Co-crystals of both domains were obtained and the complex structures were determined at 2.5–2.9 Å resolution. Based on the crystal packing of γ1-ear and the cognate peptide, γ1-ear fused with a peptide tag at the N-terminus was prepared. The peptide-tagged γ1-ear readily crystallized and the crystal diffracted far better, 1.9–2.2 Å resolution, compared with the co-crystallized complex, giving significantly more details without affecting the overall complex structure.

1. Introduction

The majority of proteins in living cells exhibit their biological functions through interactions with proteins, nucleic acids, carbohydrates, lipids and other biological molecules. Understanding their functions at atomic level thus requires structural analyses of their complexes, rather than individual molecules. Unfortunately, many protein–protein interactions are weak and transient, although specific, which makes crystallization of the complexes a formidable task. If a complex is formed by a high-affinity interaction, crystallization is easier because the complex can be purified as such and submitted to crystallization trials in a usual manner like a single polypeptide chain. However, crystallization of protein complexes with low affinities is substantially more difficult because of heterogeneous distributions of monomers and complexes in the crystallization solutions. In case of protein–peptide complexes, it is sometimes useful to add an excess amount of peptide to push the equilibrium towards the complex formation. On the other hand, it is not unusual that one of the protein (or peptide) components of the complex may be crystallized instead of the entire complex.

Fusion proteins are very useful in a broad range of biological experiments such as biochemical purification, immunodetection, functional genomics, analysis of intracellular protein transport and analysis of the protein–protein or protein–nucleic acid interactions (Beckwith, 2000). In particular, recent reports suggested that fusion proteins can be a powerful tool for structural studies of protein–protein complexes (Pellegrini *et al.*, 2002; Volkman *et al.*, 2002). Pellegrini *et al.* covalently linked a 39 amino-acid motif derived from BRCA2 to the N-terminus of RAD51 by means of the flexible 14 residues (Thr-Gly-Ser)$_4$Met-Gly designed to allow unrestrained interaction between BRCA2 and RAD51, a recombinase involved in DNA repair. This enabled purification of the RAD51–BRCA2 complex as a fusion protein, overcoming the natural tendency of RAD51 to form heterogeneous aggregates. The crystal structure of the complex was determined at 1.7 Å resolution, which shows how

the conserved BRCA2 sequence can affect the oligomerization of RAD51, thus leading to the biological implications on cancer susceptibility. Volkman and coworkers also made a stable complex by fusing a 25-residue WIP motif to the N-terminus of the N-WASP EVH1 domain *via* a five-residue linker. The complex was highly soluble and the NMR structure of the complex was determined. Although in both cases artificial amino-acid linkers might have been problematic, the flexible peptide chains they designed turned out not to disturb the interaction between the interacting partners.

Intracellular protein transport is essential for the function of eukaryotic cells. For example, correct targeting of newly synthesized glycoproteins is accomplished by a set of transport vesicles from the ER to the Golgi apparatus and then to the final destinations. The vesicular transport is controlled by an intricate network of specific but weak and transient protein–protein interactions, and therefore full understanding of their functions requires atomic details of these weakly bound complexes. The clathrin-mediated membrane traffic is such a system responsible for the protein transport from the plasma membrane and trans-Golgi network (TGN) to the endosomal/lysosomal system. Adaptor proteins such as AP complexes and the monomeric GGAs regulate this traffic process through the ARF-regulated membrane association, the recognition of the sorting signals and the recruitment of clathrin and the accessory proteins (Boehm & Bonifacino, 2001). The γ1-adaptin ear domain (referred as γ1-ear hereafter) of AP-1 complex and the homologous GAE (γ-adaptin ear) domains of GGAs are responsible for the recruitments of accessory proteins, which are so called because they modulate the functions of AP-1 complexes and GGAs in the membrane-trafficking process. γ-Synergin is one of the proteins identified as an accessory protein for γ1-ear. It contains an EH (epsin-homology) domain in its polypeptide chain, suggesting that γ-synergin might serve as a liaison between γ1-adaptin and some other unidentified proteins related to a vesicular transport although the exact function of γ-synergin has not been fully elucidated yet. Recently, γ1-ear has also been found to interact with GGA1 hinge region, which has lead to a hypothesis that AP-1 and GGAs work cooperatively in packaging a cargo protein (Doray *et al.*, 2002). These interactions are achieved through recognition of short peptide motifs with affinities of the order of 1–100 μ*M* (Mattera *et al.*, 2004; Bai *et al.*, 2004; Yamada *et al.*, in preparation; Inoue *et al.*, in preparation). Although three-dimensional structures of γ1-ear and GAE in complex with these peptides are necessary to elucidate these interactions, such low affinities have hampered the crystallization trials of complexes.

Here, we report the crystallization of γ1-ear and GGA1-GAE domains in complex with cognate peptides. Co-crystallization of these complexes was successful at an intermediate resolution when a protein sample was mixed with an excess amount of peptides for crystallization. The resulting electron density of the cognate peptides are somewhat rugged. In order to improve the situation, a peptide-fusion strategy was employed based on the crystal packing of the protein and the peptide. The peptide tags which were fused at the N-terminus of γ1-ear have significantly improved the diffraction quality of the crystals and allowed us to discuss the protein–peptide interaction in atomic detail.

Table 1
Data-collection and refinement statistics.

Values in parentheses are for the highest resolution shells.

Crystal	Co-crystal	Co-crystal	Peptide-tagged protein	Peptide-tagged protein
Protein/peptide	GGA1-GAE/GGA1 hinge	γ1-ear/GGA1 hinge	γ1-ear/GGA1 hinge	γ1-ear/γ-synergin
X-ray source	PF-AR NW12	PF-AR NW12	PF-AR NW12	PF BL18B
Wavelength (Å)	0.978	0.978	0.974	1.000
Space group	$P2_12_12_1$	$P3_121$	$P3_121$	$P3_121$
Unit-cell parameters				
a (Å)	48.0	63.7	65.2	64.0
b (Å)	69.1	63.7	65.2	64.0
c (Å)	184.8	82.4	82.8	82.3
Resolution (Å)	50.0–2.55 (2.64–2.55)	45.8–2.7 (2.80–2.70)	50.0–2.2 (2.28–2.20)	55.4–1.85 (1.92–1.85)
Observed reflections	65150	57773	110680	72087
Unique reflections	20957	5631	10861	17202
Completeness (%)	99.7 (99.2)	99.9 (99.6)	99.8 (99.9)	99.6 (99.9)
$I/\sigma(I)$	13.1 (3.6)	11.1 (3.7)	12.6 (4.5)	11.5 (3.5)
$R_{\rm merge}$ (%)	6.5 (34.5)	7.9 (50.3)	9.4 (41.4)	6.2 (41.0)
Mosaicity (°)	0.56	0.75	0.37	0.32
$B_{\rm Wilson}$ (Å^2)	54.2	75.8	36.5	22.5
Resolution (Å)	50–2.55	45.8–2.9	56.8–2.2	55.0–1.85
$R/R_{\rm free}$ (%)	24.1/28.7	24.0/27.3	20.6/23.8	19.9/23.8
No. atoms				
Protein	4107 (4 monomers)	1022	1033	1036
Solvent	122	7	88	141
R.m.s.d. from ideality				
Bond lengths (Å)	0.017	0.008	0.006	0.005
Bond angles (°)	1.78	1.35	1.30	1.37
Average *B* factor (Å^2)				
Protein	47.9	53.3	31.8	24.7
Solvent	37.5	55.3	36.0	33.6
Ramachandran plot (%)				
Most favored	83.1	79.6	89.0	92.1
Additional allowed	16.5	20.4	11.0	7.9
Generously allowed	0.5	0.0	0.0	0.0
Disallowed	0.0	0.0	0.0	0.0

2. Materials and methods

2.1. Cloning and expression

For the γ1-ear domain expression, the genes of γ1-ear containing residues 703–822 was subcloned into the *Bam*HI-*Xho*I restriction site of pGEX-4T-2 (Amersham Biosciences). For the expression of the γ-synergin peptide-tagged γ1-ear, the DNA fragment which codes the peptide (DDFGEFSLFGE) and the linker (SGG) was inserted into the *Bam*HI site of the above plasmid. To construct the GGA1 hinge peptide-tagged γ1-ear expression plasmid, the gene of γ1-ear (residues 700–822) which contains an additional *Kpn*I restriction site after the *Bam*HI restriction site, was cloned into the *Bam*HI-*Xho*I site of pGEX-4T-2. Then, the DNA fragments which codes the peptide (TGWNSFQSS) and the linker (GT) was cloned into its *Bam*HI-*Kpn*I sites. For the GGA1-GAE domain expression, the DNA fragment for residues 507–639 of human GGA1 which covers the GAE domain was cloned into pGEX-4T-2. The addition of preceding residues (507–515) to the GAE domain (residues 515–639) improved the solubility of the protein. All constructs were expressed in *Escherichia coli.* BL21.

2.2. Purification and crystallization

The γ1-ear (residue 703–822) was purified as reported previously (Nogi *et al.*, 2002). Purified γ1-ear was dialysed against 1 m*M* Tris–HCl pH 8.0 and concentrated to 27 mg ml^{-1}. Co-crystallization of

γ1-ear with the synthesized peptide from the GGA1 hinge region (SLDTGWNSFQSS) was carried out using the hanging-drop vapor-diffusion method. Crystals of the complex were grown from a 1:15 molar mixture of γ1-ear and the peptide against a reservoir containing 10%(*w*/*v*) PEG 8000, 0.2 *M* KI, 20%(*v*/*v*) glycerol and 0.1 *M* Na bicine pH 9.4 after equilibration at 277 K for 4 d.

The GST fused GGA1-GAE protein was purified with affinity chromatography using a glutathione Sepharose 4B column (Amersham Bioscience) and cleaved by thrombin. The cleaved GGA1-GAE was further purified by Superdex 75 size-exclusion column (Amersham Bioscience) in 100 m*M* NaCl and 20 m*M* Tris–HCl pH 8.0 and concentrated to 15 mg ml^{-1}. The complex of GGA1-GAE with the synthesized peptide (SLDTGWNSFQSS) was co-crystallized under 20%(*w*/*v*) PEG 3350, 120 m*M* diammonium tartrate, after equilibration at 293 K for one week. The ratio of the protein to the peptide used for the co-crystallization was 1:5.

Two peptide-tagged γ1-ear proteins were purified on a glutathione Sepharose 4B column. After washing the column with PBS, thrombin was added to remove the peptide-tagged protein from a glutathione Sepharose 4B column and the released proteins were used for the crystallization trials. Crystals of the GGA1 hinge peptide-tagged γ1-ear appeared in a reservoir containing 1.0 *M* sodium tartrate, 0.2 *M* NaCl and 0.1 *M* Tris–HCl pH 8.0 after equilibration at 289 K for 1 d. Crystals of the γ-synergin peptide-tagged γ1-ear also appeared in a reservoir containing 3.3 *M* sodium formate, 0.2 *M* NaCl, 20% glycerol and 0.1 *M* Tris–HCl pH 8.0 after equilibration at 289 K for 1 d.

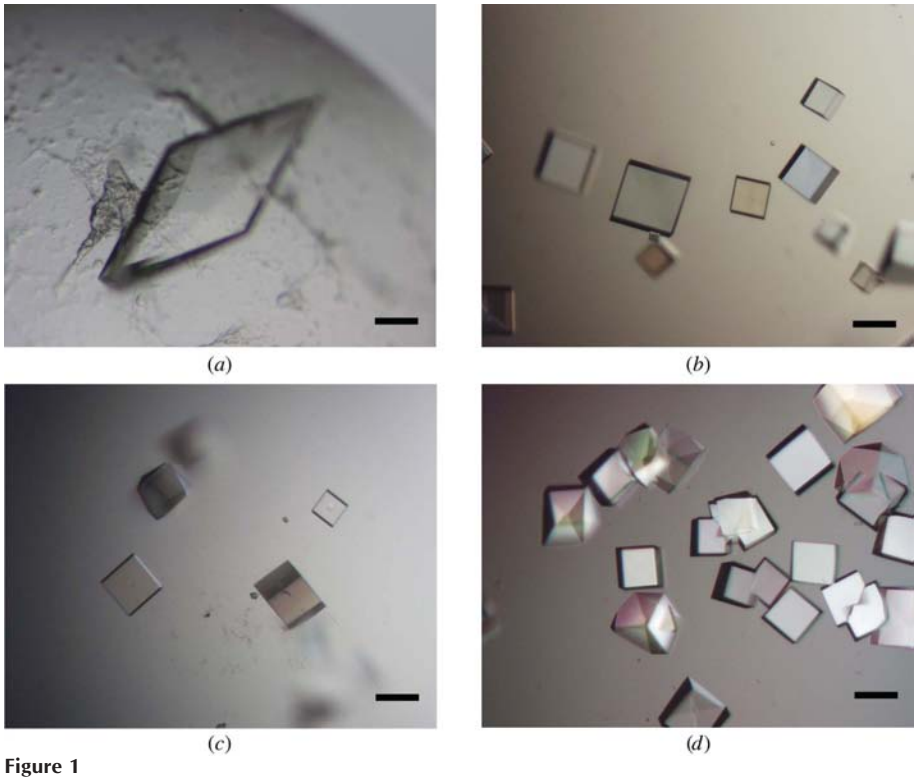

Figure 1
Crystals of γ1-ear in complex with peptides. (*a*) A co-crystal of GGA1-GAE with the GGA1 hinge peptide (*b*) co-crystals of γ1-ear with the GGA1 hinge peptide (*c*) crystal of the GGA1 hinge peptide-tagged γ1-ear (*d*) crystal of the γ-synergin peptide-tagged γ1-ear. The bars at lower right correspond to a 0.1 mm in length. Colour versions of the figures in this article are available in the online edition of the journal.

2.3. Diffraction data collection and structure determination

All data sets were collected under the cryogenic conditions. The data sets of the co-crystals of both γ1-ear and GGA1-GAE and the crystal of the GGA1 hinge peptide-tagged γ1-ear were collected at the NW12 beamline in PF-AR (Tsukuba, Japan) and processed using *HKL*2000 (Otwinowski & Minor, 1997). The data set of the crystal of the γ-synergin peptide-tagged γ1-ear was collected at the BL18B beamline in PF (Tsukuba, Japan) and processed using *HKL*2000.

All crystal structures were solved by the molecular-replacement method using program *MOLREP* (Vagin & Teplyakov,

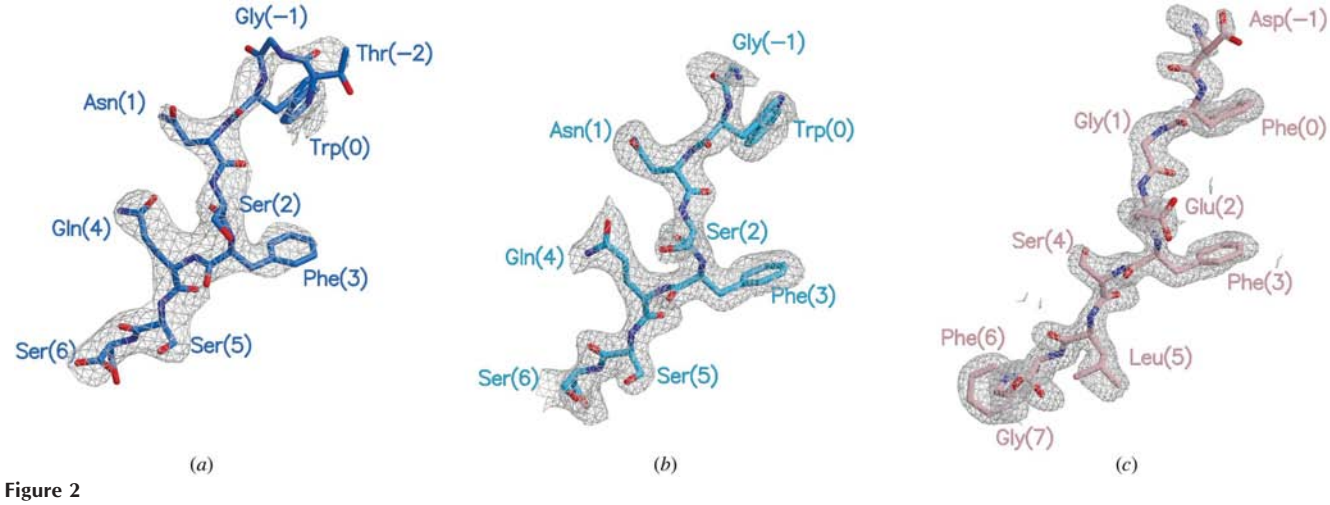

Figure 2
($F_o - F_c$) omit maps showing electron density of the cognate peptides: (*a*) co-crystal of γ1-ear with the GGA1 hinge peptide, (*b*) the crystal of the GGA1 hinge peptide-tagged γ1-ear and (*c*) that of γ-synergin peptide-tagged γ1-ear. Contour levels of the electron-density maps are 2 σ and the final models of peptides, which are represented by stick models, are superimposed.

1997) and the structure of the human γ1-ear domain as a search model (Nogi *et al.*, 2002; PDB code 1iu1). Model building was carried out with the programs *O* (Jones *et al.*, 1991) and *TURBO-FRODO* (Roussel & Cambillau, 1991) and the structures were refined using *CNS* (Brünger *et al.*, 1998) and *REFMAC*5 (Murshudov *et al.*, 1997) from *CCP*4 (Collaborative Computational Project, Number 4, 1994). Data-collection and refinement statistics are summarized in Table 1. Buried solvent-accessible surface area was calculated by *SURFACE* (Lee & Richards, 1971). Figures were prepared using *GRASP* (Nicholls *et al.*, 1991), *MOLSCRIPT* (Kraulis, 1991), *POVSCRIPT+* (Fenn *et al.*, 2003) and *RASTER3D* (Merritt & Murphy, 1994).

3. Results and discussion

3.1. Co-crystallization of γ1-ear and GGA1-GAE with peptides

The first attempt to obtain the crystal of γ1-ear in complex with the peptide was soaking the native crystal of γ1-ear in solution containing the peptide at various concentrations. However, this soaking experiment failed and no electron density corresponding to the peptides was observed. The polypeptide chain of γ1-ear we used for the native crystal contains additional 26 residues at the N-terminus, which was disordered in the crystal (Nogi *et al.*, 2002). These N-terminal residues are expected to be flexible and might drift around the binding site and block the entry of peptides to the binding site. Thus, we tried co-crystallization with a synthesized peptide by varying crystallization conditions such as crystallization reagents, protein concentration and a ratio of the protein to the peptide. Co-crystals were obtained when the protein solution was mixed with an excess amount of peptide (1:15 molar ratio). Cubic shaped co-crystals grew to a size of approximately 0.1 × 0.1 × 0.1 mm after equilibration at 277 K for 4 d (Fig. 1*b*). The crystals diffracted up to 2.7 Å resolution and a complete data set was collected. The molecular-replacement method gave us a definitive solution, which suggested that there is one γ1-ear molecule in the asymmetric unit. The co-crystal belongs to the space group $P3_121$, which is different from those reported so far for the unliganded form; the crystal structure of the unliganded γ1-ear has been solved by two groups independently (Nogi *et al.*, 2002; Kent *et al.*, 2002); the crystal reported by Nogi and coworkers belongs to $P4_32_12$ and the crystals reported by Kent and coworkers belong to $P2_12_12_1$ or $P4_12_12$. The Matthews coefficient of the co-crystal is 3.6 Å^3 Da^{-1}, corresponding to a solvent content of 66% (Matthews, 1968).

After molecular replacement, unidentified electron density was observed around four conserved basic residues Lys765, Arg793, Arg795 and Lys797, which corresponds to the putative binding site of γ1-ear (Nogi *et al.*, 2002). Although several cycles of refinements were successful in decreasing the crystallographic *R* factor to about 30%, the quality of the electron density around the binding site was not improved and it was difficult to fit a peptide model into the electron density. The final model consists of nine residues from the peptide and 122 residues from γ1-ear. The first three residues of the peptide could not be observed in the electron density map due to disorder (Fig. 2*a*).

GGA1-GAE was also co-crystallized with a synthesized peptide (the biological significance of this complex will be discussed elsewhere; Inoue *et al.*, in preparation). The binding affinities of γ1-ear and GGA1-GAE for the peptide are similar to each other; the dissociation constants are 130 and 180 μ*M*, respectively (Yamada *et al.*, in preparation; Inoue *et al.*, in preparation). In the case of GGA1-GAE, the GGA1-GAE/peptide complex were crystallized with the protein:peptide ratio of 1:5. Co-crystals grew to a size of approximately 0.3 × 0.3 × 0.6 mm after equilibrium at 293 K for a week (Fig. 1*a*) and diffracted to 2.5 Å resolution. The crystal belongs to space group $P2_12_12_1$, which is different from those of GAE/peptide crystals reported previously (Collins *et al.*, 2003; Miller *et al.*, 2003).

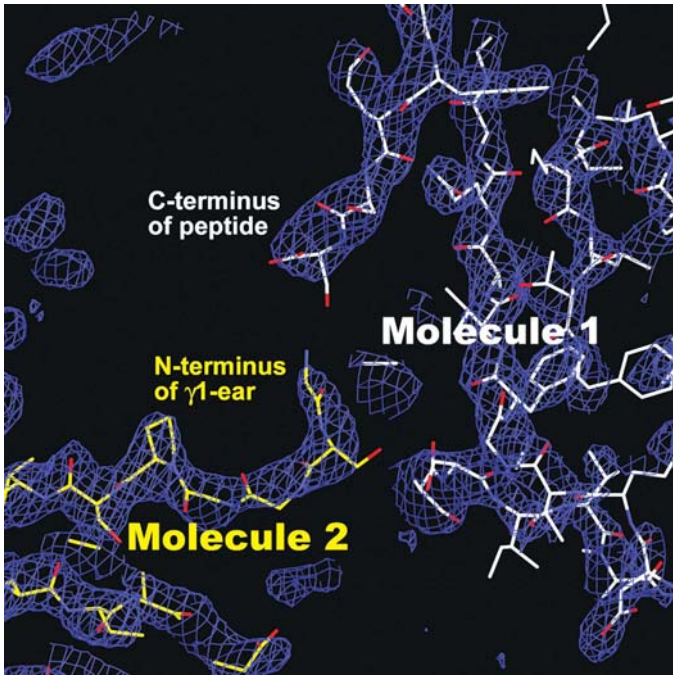

Figure 3
The $2F_o - F_c$ map around the N-terminus of γ1-ear in the co-crystal. Final model of γ1-ear/peptide complex represented by stick model is superimposed. Two molecules (1 and 2) are related by a crystallographic symmetry operation.

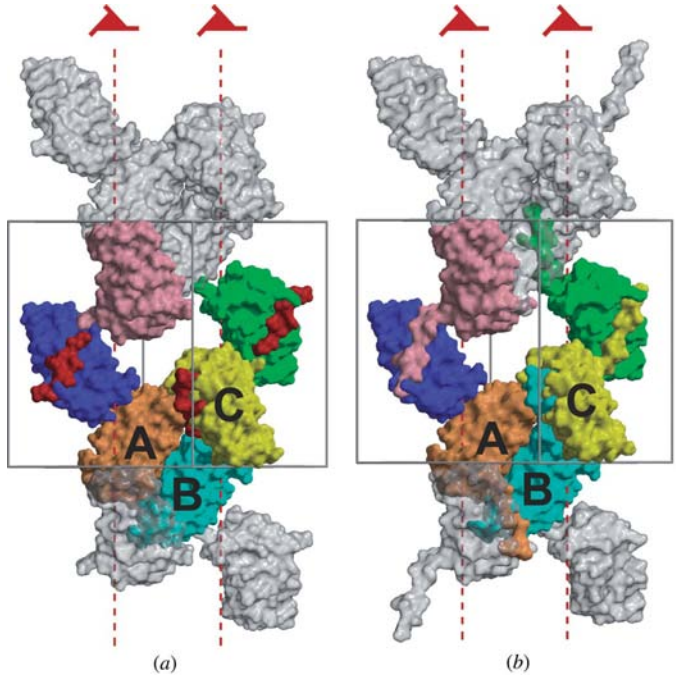

Figure 4
Molecular packing in the crystals. (*a*) and (*b*) represent the molecular packing in the co-crystal of γ1-ear with the GGA1 hinge peptide and in the crystal of the GGA1 hinge peptide-tagged γ1-ear, respectively. The solid lines represent a unit cell of each crystal and the broken lines represent the crystallographic 3_1 screw axis. Three molecules are labelled as *A*, *B* and *C*, respectively, for the convenience of the present discussion.

Although there are four copies of GGA1-GAE in the asymmetric unit, only three of the four GGA1-GAE monomers bind the peptide.

3.2. Crystallization of a peptide-tagged γ1-ear

During the refinement and model building of the γ1-ear/peptide complex using the data set from the co-crystal, we noticed that the N-terminus of γ1-ear is in the proximity of the C-terminus of the peptide that comes from a neighboring molecule related by a crystallographic symmetry operation (Fig. 3). The distance between the C^{α} atoms of these two residues is 7.0 Å. This led us to prepare a construct where the peptide was fused to the N-terminus of the γ1-ear domain. A peptide TGWNSFQSS is fused *via* a two-amino-acid linker (GT) to residues 700–822 of γ1-ear and the fusion protein was readily crystallized. Although crystals were grown from a crystallization reagent different from that of the co-crystallization after equilibration at 289 K for 1 d, their shape and size are similar to those of the co-crystals described above (Fig. 1*c*). As we expected, the crystal belongs to the same space group $P3_121$, with similar unit-cell parameters to those of the co-crystal. The crystal quality was significantly improved, with diffraction to 2.2 Å resolution. The improvement of crystal quality is also evident in the decrease of mosaicity and *B* factor as indicated by a Wilson plot (Table 1). The electron density of the peptide was remarkably improved (Fig. 2*b*), allowing us to build the peptide model easily. Owing to the improvement of the resolution, we could also include water molecules in the model and this allowed us to discuss the protein–peptide interaction including water mediated hydrogen bonds. After several cycles of refinement and manual model building, the *R* factor dropped easily to around 20%. The final model consists of almost all residues of the peptide tag, linker, γ1-ear and solvent molecules, except for the first four N-terminal residues of the peptide tag whose electron density could not be observed.

The improvement of the diffraction quality was clearly led by the peptide tag fused at the N-terminus of γ1-ear, although crystallization conditions such as protein concentration, sample purity, temperature and crystallization reagents were different between the co-crystal of γ1-ear and the crystal of the peptide-tagged γ1-ear. The peptide tag enhances the crystallization and stabilizes the molecular packing in the crystal by increasing the contact between molecules. As shown in Fig. 4, the arrangements of molecules are identical in the co-crystal and the crystal of peptide-tagged γ1-ear, both of which belong to space group $P3_121$. There are three ways of molecular contacts in both crystals termed as *A*–*B* (between the molecules related by the crystallographic twofold axis), *B*–*C* (between the molecules related by the crystallographic 3_1 screw axis) and *A*–*C*, referring to the label used in Fig. 4. The buried accessible surface area of each molecular contact upon crystallization is compared between the co-crystal and the crystal of the peptide-tagged γ1-ear (Table 2). The molecular contact *B*–*C* is smallest among the three molecular contacts in the co-crystal (312.6 $Å^2$), but increased about fivefold in the crystal of the peptide-tagged γ1-ear (1589.7 $Å^2$). This is because the peptide, now covalently linked to the protein, contributes to the significant increase in the buried accessible surface area and serves as molecular glue between the neighboring molecules in the crystal. The other molecular contacts *A*–*B* and *A*–*C* show little change. The increase of the molecular contact *B*–*C* plays an important role for the enhancement and stabilization of crystallization. The peptide tag also improves the homogeneity of the γ1-ear/peptide complex in solution. Because the affinity of the peptide against γ1-ear is low (K_d = 130 μ*M*; Yamada *et al.*, in preparation), it is possible that some γ1-ear molecules do not have the peptides bound in the co-crystal, hence the somewhat rugged electron density of the peptide. In contrast, the peptide is always around the binding site of γ1-ear during the crystallization of the peptide-tagged protein because it is anchored by a neighboring molecule. Subsequently, the local concentration of the peptide is increased and every γ1-ear can make the complex in the crystal. Multiple effects of the stabilization of the crystal and the increase of the local concentration of the peptide lead to the significant improvements in diffraction quality and the resulting electron density.

Table 2
Buried accessible surface area ($Å^2$) upon crystallization.

The labels of molecules in the crystal refer to those in Fig. 3.

	Co-crystal	Crystal of the peptide-tagged protein
A–*B* (twofold axis)	1139.8	1125.3
B–*C* (3_1 screw axis)	312.6	1589.7
A–*C*	710.2	675.9

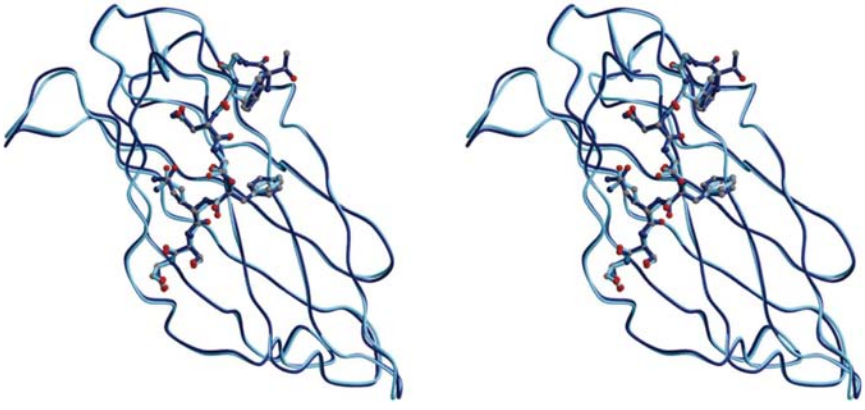

Figure 5
Stereoview showing the superposition of the structures determined from the co-crystal of γ1-ear with the peptide (dark blue) and crystal of the peptide-tagged γ1-ear (light cyan). Ribbon diagrams and ball-and-stick models represent γ1-ear and the peptide, respectively.

3.3. Comparison of the structures from the co-crystal of γ1-ear with the peptide and the crystal of the peptide-tagged γ1-ear

Although the peptide-tagged γ1-ear gave us a higher resolution structure of the complex, the covalent linkage between the peptide and the protein may disturb their interaction. To see whether there are any artificial effects on the protein–peptide interaction due to the peptide tagging, we compared the two structures from the co-crystal of γ1-ear with the peptide and the crystal of the peptide-tagged γ1-ear. Fig. 5 shows the superposition of the γ1-ear/peptide complex structures. There are very few differences in the conformation of γ1-ear and the peptide between the two structures. Root-mean-square deviations of all the atoms of γ1-ear and of the peptide are 0.68 and 0.48 Å, respectively. From these observations, we conclude that the structure of the γ1-ear/peptide complex determined by crystallization of the peptide-tagged γ1-ear reflects well the true interaction between γ1-ear and its target protein.

Based on the experience described here, we also solved the structure of the complex with a peptide derived from γ-synergin, another γ1-ear

binding protein. The peptide contains a sequence DDFGEFSLFGE, which corresponds to residues 668–677 of γ-synergin, a linker SGGGS and γ1-ear residues 703–812. This linker is different from and more flexible than that of the previous case (GT). Although crystallization reagents were different from those of the other two proteins, similar cubic shaped crystals were obtained within a day (Fig. 1*d*). The crystal belongs to the same space group $P3_121$ as that of the GGA1 hinge peptide-tagged crystals and diffracted up to 1.85 Å resolution (Table 1). The resulting electron density was very clear (Fig. 2*c*) and this enabled us to discuss the γ1-ear/peptide interaction in the atomic level and propose a new consensus motif for the γ1-ear binding (Yamada *et al.*, in preparation). Interestingly, electron density could not be observed for the glutamate (after Gly7 in Fig. 2*c*) at the C-terminus of the peptide tag due to disorder in the linker. This flexibility also supports the notion that the conformation of the peptide is free from the artificial effect of covalent linker.

We have shown that peptide tagging is a very powerful method for crystallographic studies of weakly interacting protein complexes. In our study, the prior knowledge of the crystal packing of γ1-ear in complex with the cognate peptide was used to design peptide-tagged proteins so that the peptide can bind to a neighbouring γ1-ear. However, this method can be extended to complexes whose molecular packing in a crystal is unknown *a priori*. For complexes of two large proteins where both N- and C-terminus are far away from the contact interface, one might utilize a linker long enough to make a complex of the two proteins from the same single polypeptide chain. For example, in the crystallographic study of the RAD51–BRCA2 complex, a 25-residue linker connects the C-terminus of BRCA2 and N-terminus of RAD51, whose distance is about 25 Å (Pellegrini *et al.*, 2002). In other cases a short linker might be able to form a complex of two proteins from neighboring molecules in the crystal (subunit swapping). This is similar to the current work, where the peptide tag is recognized by a neighboring molecule related by a crystallographic symmetry operation (3_1 screw axis). With a finite number of constructs to explore, such as the length of a linker and the position of the peptide tag (N-terminus or C-terminus), the peptide-tagging method is worth trying for difficult cases of crystallization of protein–protein or protein–peptide complexes whose interactions are specific but either weak or transient.

The authors thank beamline staff of Photon Factory and SPring-8. This work was supported by The National Project on Protein Structural and Functional Analyses (Priority Research Program, Protein 3000 Project) from the Ministry of Education, Culture, Sports, Science and Technology of Japan.

References

Bai, H., Doray, B. & Kornfeld, S. (2004). *J. Biol. Chem.* **279**, 17411–17417.
Beckwith, J. (2000). *Methods Enzymol.* **326**, 3–7.
Boehm, M. & Bonifacino, J. S. (2001). *Mol. Biol. Cell*, **12**, 2907–2920.
Brünger, A. T., Adams, P. D., Clore, G. M., DeLano, W. L., Gros, P., Grosse-Kunstleve, R. W., Jiang, J.-S., Kuszewski, J., Nilges, M., Pannu, N. S., Read, R. J., Rice, L. M., Simonson, T. & Warren, G. L. (1998). *Acta Cryst.* D**54**, 905–921.
Collaborative Computational Project, Number 4 (1994). *Acta Cryst.* D**50**, 760–763.
Collins, B. M., Praefcke, G. J. K., Robinson, M. S. & Owen, D. J. (2003). *Nature Struct. Biol.* **10**, 599–606.
Doray, B., Ghosh, P., Griffith, J., Geuze, H. J. & Kornfeld, S. (2002). *Science*, **297**, 1700–1703.
Fenn, T. D., Ringe, D. & Petsko, G. A. (2003). *J. Appl. Cryst.* **36**, 944–947.
Jones, T. A., Zou, J.-Y., Cowan, S. W. & Kjeldgaard, M. (1991). *Acta Cryst.* A**47**, 110–119.
Kent, H. M., McMahon, H. T., Evans, P. R., Benmerah, A. & Owen, D. J. (2002). *Structure*, **10**, 1139–1148.
Kraulis, P. J. (1991). *J. Appl. Cryst.* **24**, 946–950.
Lee, B. & Richards, F. M. (1971). *J. Mol. Biol.* **55**, 379–400.
Mattera, R., Ritter, B., Sidhu, S. S., McPherson, P. S. & Bonifacino, J. S. (2004). *J. Biol. Chem.* **279**, 8018–8028.
Matthews, B. W. (1968). *J. Mol. Biol.* **33**, 491–497.
Merritt, E. A. & Murphy, M. E. P. (1994). *Acta Cryst.* D**50**, 869–873.
Miller, G. J., Mattera, R., Bonifacino, J. S. & Hurley, J. H. (2003). *Nature Struct. Biol.* **10**, 607–613.
Murshudov, G. N., Vagin, A. & Dodson, E. J. (1997). *Acta Cryst.* D**53**, 240–255.
Nicholls, A., Sharp, K. & Honing, B. (1991). *Proteins Struct. Funct. Genet.* **11**, 281–296.
Nogi, T., Shiba, Y., Kawasaki, M., Shiba, T., Matsugaki, N., Igarashi, N., Suzuki, M., Kato, R., Takatsu, H., Nakayama, K. & Wakatsuki, S. (2002). *Nature Struct. Biol.* **9**, 527–531.
Otwinowski, Z. & Minor, W. (1997). *Methods Enzymol.* **276**, 307–326.
Page, L. J., Sowerby, P. J., Lui, W. W. & Robinson, M. S. (1999). *J. Cell. Biol.* **146**, 993–1004.
Pellegrini, L., Yu, D. S., Lo, T., Anand, S., Lee, M., Blundell, T. L. & Venkitaraman, A. R. (2002). *Nature (London)*, **420**, 287–293.
Roussel, A. & Cambillau, C. (1991). *Silicon Graphics Geometry Partners Directory*. Mountain View, CA, USA: Silicon Graphics.
Vagin, A. & Teplyakov, A. (1997). *J. Appl. Cryst.* **30**, 1022–1025.
Volkman, B. F., Prehoda, K. E., Scott, J. A., Peterson, F. C. & Lim, W. A. (2002). *Cell*, **111**, 565–576.